Toward Safer Neurosurgery with an Active Handheld Instrument

F. Prudente[1], S. Moccia[1,2], A. Perin[3], R. F. Sekula[4], L. S. Mattos[2], J. R. Balzer[4], W. Fellows-Mayle[4], E. De Momi[1], C. N. Riviere[5]

[1]*Dept. of Electronics, Information and Bioengineering, Politecnico di Milano, Milan, Italy*
[2]*Department of Advanced Robotics, Istituto Italiano di Tecnologia, Genoa, Italy*
[3]*Besta NeuroSim Center, IRCCS Istituto Neurologico C. Besta, Milan, Italy*
[4]*Department of Neurological Surgery, University of Pittsburgh, Pittsburgh, USA*
[5]*Robotics Institute, Carnegie Mellon University, Pittsburgh, USA*
francesca.prudente@mail.polimi.it, sara.moccia@polimi.it

INTRODUCTION

Improvements in microsurgical dissection techniques, skull base approaches, imaging modalities, and intraoperative neurophysiologic monitoring have led to a reduction in surgical morbidity and mortality for deep-seated brain tumors and cerebrovascular lesions. Despite these improvements, however, postoperative rates of cerebral infarction and cranial nerve deficits remain high and dramatically reduce quality of life in patients with a variety of brain disorders [1], [2]. In the case of petroclival meningioma, for example, the incidence of permanent cranial nerve deficits is between 20% to 76% while gross total resection is achieved in only 20% to 85% of patients [3]. An assist device that would allow the surgeon to reduce larger unintended movements, automatically avoiding sensitive tissues, may result in reduced morbidity for patients [4].

MATERIALS AND METHODS

This work consists of three main steps: (i) vessel segmentation, (ii) 3D reconstruction and (iii) implementation of the forbidden-region VF framework.

Segmentation Algorithm

A Geometrical Deformable Model (GDM)-based approach is used to perform vessel segmentation [5]. The vessel segmentation algorithm requires as initialization the manual selection of a starting point p_1 and an ending point p_2, which are then automatically connected with a minimal-cost path algorithm. The resulting path is used as initialization of the GDM algorithm. The deformation of the GDM is guided by intensity-based external forces, which are retrieved from the *vesselness* measures defined in [6].

3D Reconstruction Algorithm

The 3D reconstruction is performed in order to extract the 3D position of the segmented vessel surface in the Micron control reference system. Micron is a 6-DOF handheld instrument equipped with piezoelectric actuators so that its tip can move semi-independently of the hand motion (range of motion: Ø4.0 × 4.0 mm) [7]. The Micron system setup (Fig. 1) includes (i) an optical tracker (Apparatus to Sense Accuracy of Position (ASAP)) for tracking Micron tip position, and (ii) a stereo operating microscope (Zeiss OPMI, Carl Zeiss, AG, Germany) equipped with two CCD cameras (f=30 Hz, 800x600 pixels). Since the controller of Micron works in the ASAP reference system while the target is detected by the stereo-cameras, calibration mappings are mandatory. A laser probe integrated into Micron is used to scan the surface, since the camera calibration must match a set of 3D tip positions measured by the ASAP with a set of 2D locations detected in the camera images [8]. For the 3D reconstruction, the Speeded Up Robust Features (SURF) detection algorithm is used [9]. The point cloud relative to the vessel position is retrieved by applying the sum-of-squared-distance-ray tracing method to corresponding point pairs. The vessel surface is reconstructed exploiting the convex hull, a triangular mesh that encompasses the retrieved point cloud.

Forbidden-Region Virtual Fixtures

The forbidden-region VF implements the vessel collision avoidance task, preventing the manipulator to enter into a predefined avoidance zone, representing the segmented vessel and a cylindrical safety zone surrounding it.

The control command is triggered as soon as the distance d between the tool tip and the vessel surface becomes lower than the cylindrical radius. Each time a new tip position sample is detected by ASAP, the algorithm finds the closest point p_s belonging to the vessel surface and computes d. The *Micron* tip is driven to reach a point distant d_{safety} (i.e. the cylindrical radius) from p_s if d is less than d_{safety}.

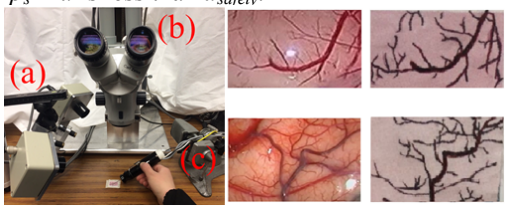

Fig. 1 On the left the system set-up: (a) ASAP tracking system; (b) Zeiss stereo operating microscope; (c) Micron manipulator. On the right orginal video frames and examples of printed pattern.

Experimental Protocol

The vessel segmentation algorithm was tested on fifty microscopy video frames acquired during two neurosurgical interventions at Istituto Neurologico Carlo Besta. The segmentation algorithm was evaluated

in terms of accuracy, sensitivity, specificity and Dice similarity coefficient, computed with respect to gold-standard manual segmentation performed by an expert.

For the VF performance evaluation, an experimental setup was developed to simulate the surgical environment and let Micron interact with phantom vessels. Three flat patterns that reproduce the vessels to avoid were printed (Fig.1). Twenty-one images of these patterns (seven of each pattern) with different orientations were captured by the left and the right camera of the Micron microscope (4× magnification). The accuracy of the 3D reconstruction was evaluated in terms of reprojection errors of the point cloud.

The vessel avoidance algorithm was tested in real time by operating Micron above an image of the vascular pattern and making repeated attempts to cross the blood vessel while in contact with the surface.

RESULTS

Vessel segmentation performance values are reported in Table 1. The reprojection error statistics computed for the 21 phantom images are shown in Table 2.

Table 1. Segmentation algorithm performance

	q_1	$\tilde{x}$	q_2	IQR
Acc	0.999	0.999	0.999	4.0e-04
Se	0.701	0.761	0.819	0.119
Sp	0.999	0.999	0.999	2.0e-04
DSC	0.796	0.8329	0.849	0.053

Acc=Accuracy; Se=Sensitivity; Sp=Specificity; DSC=Dice Similarity Coefficient; q_1= 1st quartile; $\tilde{x}$=median; q_3= 3rd quartile; IQR=Interquartile Range

Table 2. Reprojection error distribution for 21 phantom images

images	q_1	$\tilde{x}$	q_2	IQR
left	0.6791	0.8890	1.4158	0.7367
right	0.6901	0.8992	1.4276	0.7375

q_1= 1st quartile; $\tilde{x}$=median; q_3= 3rd quartile; IQR=Interquartile Range

Using the VF algorithm, the Micron tip was forced to lift over the vessel (green trajectory in Fig. 2) when the null position of the manipulator (red trajectory in Fig. 2) was within d_{safety} = 1.6 mm. The d measure over time when the VF is active (green) is plotted in Fig. 3 against what the distance would have been if the VF were inactive (red).

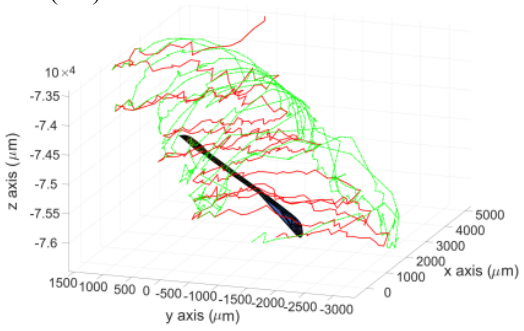

Fig. 2 Automatic avoidance of vessel (black). The Micron tip trajectories are shown for when the Virtual Fixtures are on (green) and off (red).

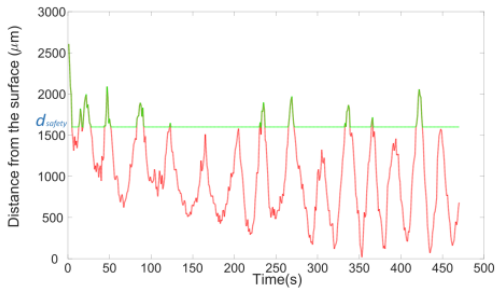

Fig. 3 Distance, d, of the Micron tip from the vessel surface over time when the Virtual Fixture is on (green) *vs*. what it would have been if the fixture were off (red). d_{safety} is the chosen safety distance (1600 μm).

DISCUSSION

In this paper, we presented a new approach to vessel avoidance for safe robotic assisted neurosurgery, which exploits an actuated handheld tool to reliably constrain penetration into predefined forbidden zones. Future work will aim at implementing a tracking algorithm for real-time applications in order to take into account also tissue deformation and the presence of surgical tools in the scene, which can eventually occlude the vessel to be avoided. A 3D phantom that reproduces a more truthful surgical scenario will be further developed for testing.

ACKNOWLEDGMENTS

Partial funding provided by U.S. National Institutes of Health (grant no. R01EB000526) and by Politecnico di Milano, Italy.

REFERENCES

[1] Lawrence JD et al. An investigation into quality of life improvement in patients undergoing microvascular decompression for hemifacial spasm. Journal of Neurosurgery. 2017; 1-9.

[2] Sekula RF et al. Microvascular decompression for hemifacial spasm in patients> 65 years of age: an analysis of outcomes and complications. Muscle & nerve. 2013; 48(5): 770-776.

[3] Xu F et al. Petroclival meningiomas: an update on surgical approaches, decision making, and treatment results. Neurosurgical focus. 2013; 35(6): E11.

[4] Trope M et al. The role of automatic computer-aided surgical trajectory planning in improving the expected safety of stereotactic neurosurgery. Int J Comput Assist Radiol Surg. 2015;10(7):1127-40.

[5] Moccia S et al. Safety enhancement in robotic neurosurgery through vessel tracking. Proc 6th Joint Workshop on New Technologies for Computer/Robot Assisted Surgery. 2016.

[6] Frangi AF et al. Multiscale vessel enhancement filtering. Med Image Comput Comput Assist Interv. 1998;130-7.

[7] Yang S et al. Manipulator design and operation for a six-degree-of-freedom handheld tremor-canceling microsurgical instrument. IEEE/ASME Trans Mechatron. 2015; 20(2):761-72.

[8] Yang, S. Handheld micromanipulator for robot-assisted microsurgery. Ph.D. dissertation, Carnegie Mellon Univ. 2015.

[9] Bay H et al. Speeded-up robust features (SURF). Comput Vis Image Understanding. 2008;110:346-59.